EFFECT OF SINTERING TEMPERATURE ON THE MICROSTRUCTURE AND PROPERTIES OF POWDER METALLURGY $Hf_{0.5}Nb_{0.5}Ta_{0.5}Ti_{1.5}Zr$ REFRACTORY HIGH-ENTROPY ALLOY

Larissa A. GOUVEA[1], Zuzana KOVACOVA[2], Vit JAN[1], Zdenek SPOTZ[1], Michael KITZMANTEL[2], Erich NEUBAUER[2], Ivo DLOUHY[1]

[1]Brno University of Technology, Faculty of Mechanical Engineering, Institute of Materials Science and Engineering, NETME centre, Brno, Czech Republic, EU, gouvea@fme.vutbr.cz

[2]RHP-Technology GmbH, Forschungs- und Technologiezentrum, Seibersdorf, Austria, EU

https://doi.org/10.37904/metal.2019.935

Abstract

The present work is focused on the synthesis and mechanical properties evaluation of non-equiatomic $Hf_{0.5}Nb_{0.5}Ta_{0.5}Ti_{1.5}Zr$ Refractory High-Entropy Alloy (RHEA). For the alloy production, a combination of mechanical alloying (MA) process in a planetary ball mill and hot pressing (HP) for powder densification was utilized. The effect of different sintering temperatures was explored in a temperature range of 1200 °C up to 1600 °C. The bulk material was then subject to investigation in terms of its microstructural features, elemental and phase composition and basic mechanical properties by scanning electron microscopy (SEM), X-ray diffraction (XRD), as well as hardness testing, density determination by Archimedes' principle. The results show that very hard fine grained bulk materials were achieved in all microstructures, with an average hardness of (784 ± 5) HV0.2, (793 ± 3) HV0.2 and (814 ± 5) HV0.2 for the sintering temperatures of 1200 °C, 1300 °C and 1600 °C respectively. The slightly minimum increase in hardness might be attributed to the partial dissolution of a second-phase triggered by the increase in temperature.

Keywords: Compositionally complex alloys, refractory alloy, hot pressing, mechanical alloying

1. INTRODUCTION

A new alloy design strategy called high-entropy alloys (HEAs) has attracted significant attention from the scientific community in the past decade [1] due to the unique properties that one could achieve by alloying multi-principal elements in equal or near-equal atomic ratios [2,3]. Following the same strategy, by a careful selection of elements from the groups IV, V and VI, the exploration of a subclass of alloys can be examined: refractory high-entropy alloys (RHEAs).

RHEAs are promising candidates for a new-generation of high temperature materials derived from their high melting points, ability to achieve high-temperature strength and the claimed slow diffusion kinetics [4-6], even exhibiting superior high-temperature performance compared to some commercial nickel-base superalloys at elevated temperatures [5,7]. However, they generally suffer from room temperature brittleness [5,8], but recent efforts on ductilizing RHEAs utilizing strategies like phase transformation, electron theory - including transformation-induced plasticity effect -, first principle calculations using ab initio alloy theory (to predict alloying effect on the micro-mechanical level on the elastic properties and tensile strength of BCC RHEAs), indicate that ductilization is possible [9-12]. More specifically, the $Hf_{0.5}Nb_{0.5}Ta_{0.5}Ti_{1.5}Zr$ RHEA has been shown to possess promising properties, such as ductility at room and high-temperatures combined with high-strength [10,13] in the cast states.

In this paper, results on the characterization of a RHEA ($Hf_{0.5}Nb_{0.5}Ta_{0.5}Ti_{1.5}Zr$) produced by a combination of mechanical alloying and hot uniaxial pressing are presented, and a comparison of the effect of three different sintering temperatures (1200, 1300 and 1600 °C) into the microstructural characterization and basic mechanical properties is reported.

2. MATERIALS AND METHODS

The powder preparation was done by firstly reducing Zr sponge - commercial purity of 99 % into powder in a hardened steel milling bowl filled with high purity argon atmosphere together with hardened bearing steel balls (100Cr6) of 20 mm and 15 mm diameter (1:1 ratio of the diameter of the balls), in a 10:1 ball-to-powder weight ratio (BPR) for 6 h in ethanol. The powders were dried in argon atmosphere. After the first milling, powders of Hf, Nb, Ta and Ti - with commercial purity of 99.95 % - were further added in the milling bowl together with the prepared Zr powder and hardened steel balls of 15 mm diameter, in a 10:1 BPR. The bowl was filled again with high-purity argon atmosphere. The sealed bowl was introduced into a planetary ball mill (Fritsch Pulverisette 6). The milling was conducted for a total of 10 h in a speed of 250 rpm, in a set time schedule of 15 min milling and 1 h idle, for 40 cycles. After the milling, ethanol was added and wet milling has been performed for extra 20 min for a complete removal of the powders from the surfaces. The powder manipulation was all performed in argon-filled glovebox.

The sintering was performed by Hot Pressing (HP) in vacuum atmosphere at a constant uniaxial pressure of 50 MPa applied by die pistons. For the reduction of potential surface contamination, boron nitride coating was used on the graphite die. Different sintering temperatures were used for the same feedstock powders, sequentially named as RHEA_1200ºC, RHEA_1300ºC, RHEA_1600ºC. The sintering was carried out for all alloys at a heating rate of 100 ºC.min^{-1} up to 50 ºC from the maximum sintering temperatures. On the last 50 ºC, a heating rate of 25 ºC.min^{-1} was used with a dwell time of 10 min. After the sintering process, the whole machine setup was left to cool slowly in the vacuum chamber for every sample.

The resulting bulk specimens were approximately 6 mm high with 15 mm diameter in a cylindrical shape. The samples were analysed by SEM (Zeiss Ultra Plus) utilizing energy-dispersive X-ray spectroscopy (EDS). The constituent phases were analysed based on the acquired XRD spectra, obtained using the diffractometer Philips X'Pert, operated under the voltage of 40 kV with current of 30 mA. A continuous scanning was performed with 2θ between 10° and 100° using a speed of 0.02 °/min and step size of 0.0167°. The radiation used was Cu-Kα with λ = 0.154056 nm.

The density of the alloys was determined by the Archimedes' principle. Vickers hardness measurements were carried out using a load of 200 g, as well as dwell time of 10 s on the polished samples (15 measurements) using LM 247AT microhardness tester.

3. RESULTS AND DISCUSSION

The XRD pattern analysis of the powder metallurgy $Hf_{0.5}Nb_{0.5}Ta_{0.5}Ti_{1.5}Zr$ bulk is shown in **Figure 1**. The two main phases are BCC-based with an additional third HCP phase. Furthermore, oxides and carbide-like phases are present.

The analysis on RHEA_1200 ºC showed that the matrix is a body-centered cubic structure and possesses a calculated volume fraction of 35.5 %. The second phase is a BCC-solid solution with a volume fraction of 24.9 %. The alloy contains also small HCP precipitates in 4.8 % vol. and presence of a carbide-like structure as 27.2 % in volume. Additionally, the RHEA formed oxides within a volume fraction of 5.1 %.

RHEA_1300 ºC showed a similar trend, except for the lack in formation of oxides. The alloy has a BCC matrix with 38.8 % vol., a BCC-solid solution as second-phase with 27.0 % vol., presence of HCP precipitates in 14 % - the amount increased with an increase in temperature. The carbide-like phase is also present in a smaller volume: 15.7 %.

As for RHEA_1600 ºC, the bulk showed the same BCC matrix with 37.9 vol%, second-phase BCC solid-solution with 21.4 vol%, the HCP precipitates continuously increased with the rise in temperature, possessing a volume fraction of 28.4 %.

The decrease in the carbide-like precipitation with increase in temperature suggests a change in solubility of the phase, where the partial dissolution of the carbides is thermodynamically favourable - the amount decreased from 27.2 % down to 9.3 %. On the other hand, the HCP precipitation is favoured with the rise in temperature, with an increase from 4.8 % up to 28.4 %.

The oxide formation only takes place at 1200 ºC, suggesting that, at sintering temperatures above this value, the mentioned particles might dissolve partially or fully, as there was no detection of the same oxide crystals in XRD due to the limited detection threshold.

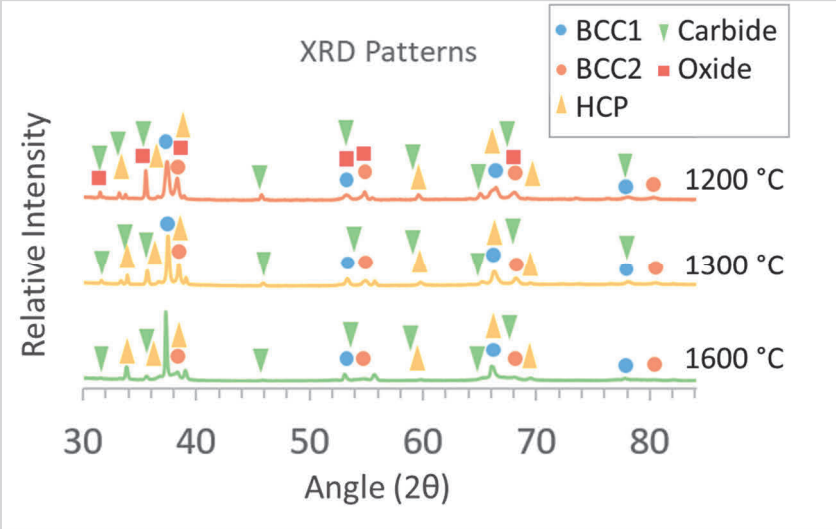

Figure 1 XRD Pattern of the Hf0.5Nb0.5Ta0.5Ti1.5Zr

These results might suggest that different manufacturing methods may produce different microstructures in the non-equiatomic $Hf_{0.5}Nb_{0.5}Ta_{0.5}Ti_{1.5}Zr$. The powder metallurgy alloys produced by this work are reported in the as-sintered state as dual BCC microstructures with additional HCP precipitates and presence of oxides/carbides inherently attributed to the mechanical milling process [14-17].

The $Hf_{0.5}Nb_{0.5}Ta_{0.5}Ti_{1.5}Zr$ arc-melted RHEAs have been reported to show a single BCC-solid solution [10,13], even after annealing at 900 °C for 14 days [13]. At 800 °C annealing for 14 days, however, the same RHEA has been reported to possess a small fraction of second-phase BCC precipitates at the grain boundaries. After annealing at 500 °C, nonetheless, a more complex microstructure was achieved, consisting of 2 BCCs and HCP phases [13] - similarly to the results obtained by the present work already in the as-sintered state.

The microstructures of RHEA subjected to different sintering temperatures can be observed in **Figure 2**. The complementary EDS point analysis is presented in **Table 1**. The matrix is designated as BCC1 and it is Ti-, Zr- rich and the second-phase BCC-solid solution (BCC2 - Zr-,Hf- rich) nucleates in the grain boundaries of the matrix for all alloys (**Figure 2**). The HCP precipitation occurs in the vicinity of the BCC2 particles for all alloys, as it is shown in **Figures a.1., b.1., c.1**.

One can notice that with the decrease in temperature from 1600 °C to 1200 °C, a significant grain refinement takes place and the microstructure becomes more complex, where, at 1200 °C, O- and Hf- rich particles become evident (**Figure 1.a.** and **Table 1**). The composition of the BCC1 matrix and BCC2 second-phase are very similar for all alloys as it can be compared in **Table 1**.

Moreover, in **Figure 2.d**, one can observe the overlapped mapping of all elements (Nb, Zr, Ta, Hf, Ti) performed by EDS on the cross-section of the milled powders. It is clear that 10 h milling was sufficient for a homogeneous mechanical mixing of the elements. Any potential segregation on the final microstructure of the bulk alloys is not a consequence of the mechanical milling.

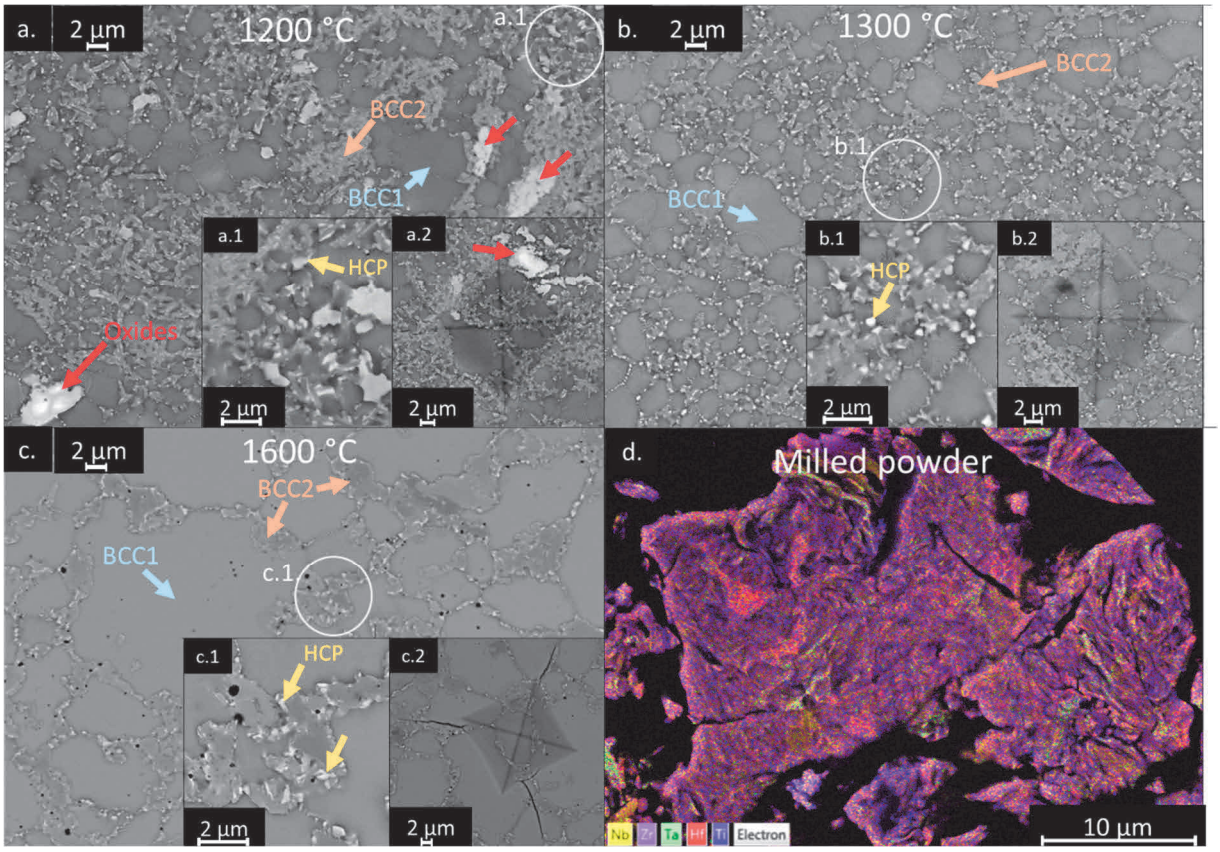

Figure 2 Micrographs of Hf0.5Nb0.5Ta0.5Ti1.5Zr with highlighted major phases: a) RHEA_1200ºC - a.1. highlighted HCP phase; a.2. microindent without crack; b) RHEA_1300ºC - b.1 highlighted HCP phase; b.2. microindent without crack; c) RHEA_1600ºC - c.1. highlighted HCP phase along the grain boundaries; c.2. microindent with cracks; d) EDS mapping of the cross-section of the milled powders

Table 1 EDS point analysis' results of each phase encountered in the micrographs on the RHEAs

	1200 ºC			1300 ºC		1600 ºC	
	BCC1	**BCC2**	**Oxide**	**BCC1**	**BCC2**	**BCC1**	**BCC2**
Ti	46.0 ± 0.9	20.1 ± 2.9	2.9 ± 0.7	43.5 ± 0.4	19.3 ± 0.3	42.8 ± 0.1	15.1 ± 0.8
Zr	19.1 ± 0.4	38.9 ± 2.3	-	18.2 ± 0.5	40.5 ± 0.5	18.7 ± 0.3	46.6 ± 1.3
Nb	11.9 ± 1.1	5.3 ± 0.3	-	13.4 ± 0.2	4.7 ± 0.2	13.5 ± 0.1	2.4 ± 0.6
Hf	10.9 ± 0.4	28.4 ± 0.8	35.4 ± 0.2	9.6 ± 0.1	29.0 ± 0.1	10.2 ± 0.1	31.1 ± 0.7
Ta	12.3 ± 0.7	7.3 ± 0.1	1.6 ± 0.3	15.4 ± 0.8	6.6 ± 0.1	14.8 ± 0.1	4.9 ± 0.7
O	-	-	60.2 ± 0.8	-	-	-	-

In **Table 2**, the basic mechanical properties of the $Hf_{0.5}Nb_{0.5}Ta_{0.5}Ti_{1.5}Zr$ samples are presented. The average hardness and density for all sintering conditions are very similar, respectively possessing (789.6 ± 5.3) HV and 8.13 g.cm^{-3} for RHEA_1200 °C, (795.7 ± 3.3) HV and 8.15 g.cm^{-3} for RHEA_1300 °C and (814.2 ± 5.1) HV and 8.16 g.cm^{-3} for RHEA_1600 °C. On the other hand, the same alloy produced in as-cast condition is 301 HV and possesses density of 8.13 g.cm^{-3} [10]. The much higher hardness is attributed to the multiple-phase microstructure in the PM alloys, in contrast with a single-phase BCC for casting. The density is analogous for both manufacturing routes due to the attainment of full density in our samples, which can be comparable to those of current Ni-based superalloys.

Table 2 Comparison of the mechanical properties of the studied RHEAs: Vickers hardness and density.

Sample	**Hardness** (HV 0.2)	**Theoretical density** ($g.cm^{-3}$)	**Archimedes density** ($g.cm^{-3}$)	**% density**
RHEA_1200 ºC	789.6 ± 5.3	8.17	8.13	99.5 %
RHEA_1300 ºC	795.7 ± 3.3	8.17	8.15	99.8 %
RHEA_1600 ºC	814.2 ± 5.1	8.17	8.16	99.9 %

One can perceive that a slight increase in hardness with increasing temperature for the PM alloys might be a consequence of the increasing amount of HCP precipitates for higher temperatures of sintering. On the other hand, a partial dissolution of carbide-like precipitate triggered by the increase in temperature is taking place.

The highest temperature of sintering also seems to decrease the fracture resistance of the material, as it can be noticed in **Figure 2.a.2** and **2.b.2**, at 1200 °C and 1300 °C, respectively. The indents do not cause any crack propagation. However, for 1600 °C (**Figure 2.c.2**) crack propagation is evident on the indents.

4. CONCLUSION

In this paper, the $Hf_{0.5}Nb_{0.5}Ta_{0.5}Ti_{1.5}Zr$ refractory high-entropy alloy was prepared by a combination of mechanical alloying and HP. The major conclusions of the work are drawn as follows:

- The as-sintered RHEA produced by PM can achieve a multiple-phase microstructure (2 BCCs, HCP and oxides/carbides) in contrast with the as-cast state single BCC alloy [10, 13].
- Dissolution of carbides is thermodynamically favorable with increasing the sintering temperature from 1200 ºC to 1600 ºC (37 % from the total volume of carbides were dissolved). At the same time, significant increase in volume fraction of HCP precipitates in the $Hf_{0.5}Nb_{0.5}Ta_{0.5}Ti_{1.5}Zr$ is observed with the rise in temperature.
- The increasing in sintering temperature is directly proportional to the increasing in hardness. Nonetheless, the hardness increase is minimum, even though the material seems to embrittle.
- The PM route produces an increase in hardness of more than double as compared to the same alloy produced by cast as previously reported in the literature (301 HV - as-cast) [10].
- The oxides formation on the refractory high-entropy alloy $Hf_{0.5}Nb_{0.5}Ta_{0.5}Ti_{1.5}Zr$ produced by powder metallurgy may be explored as a route for producing ODS RHEAs.

ACKNOWLEDGEMENTS

This research has been supported by the research project no. 19-22016S of Czech Science Foundation. The project no. FSI-S-17-4711 of Brno University of Technology is further acknowledged.

REFERENCES

[1] MURTY, B.S., YEH, J.W. and RANGANATHAN, S. *High-Entropy Alloys*. 2014. 204 p.

[2] YEH, J.W., CHEN, S.K., LIN, S.J., GAN, J.Y., CHIN, T.S., SHUN, T.T., TSAU, C.H. and S.Y. CHANG, Nanostructured high-entropy alloys with multiple principal elements: Novel alloy design concepts and outcomes, *Advanced Engineering Materials*. 2004. vol. 6, no. 5, pp. 299-303.

[3] CANTOR, B., CHANG, I.T.H., KNIGHT, P. and VINCENT, A.J.B. Microstructural development in equiatomic multicomponent alloys. *Materials Science and Engineering: A*. 2004. vol. 375-377, pp. 213-218.

[4] MIRACLE, D.B. and SENKOV, O.N. A critical review of high entropy alloys and related concepts. *Acta Materialia*. 2017. vol. 122, pp. 448-511.

[5] SENKOV, O.N., WILKS, G.B., MIRACLE, D.B., CHUANG, C.P. and LIAW, P.K. Refractory high-entropy alloys. *Intermetallics*. 2010. vol. 18, no. 9, pp. 1758-1765.

[6] LU, Z.P., WANG, H., CHEN, M.W., BAKER, I., YEH, J.W., LIU, C.T. and NIEH, T.G. An assessment on the future development of high-entropy alloys: Summary from a recent workshop. *Intermetallics*. 2015. vol. 66, pp. 67-76.

[7] SENKOV, O.N., SCOTT, J.M., SENKOVA, S.V., MEISENKOTHEN, F., MIRACLE, D.B. and WOODWARD, C.F. Microstructure and elevated temperature properties of a refractory TaNbHfZrTi alloy. *Journal of Materials Science*. 2012. vol. 47, no. 9, pp. 4062-4074.

[8] SENKOV, O.N., WILKS, G.B., SCOTT, J.M. and MIRACLE, D.B. Mechanical properties of Nb25Mo25Ta25W25 and V20Nb20Mo20Ta20W20 refractory high entropy alloys. *Intermetallics*. 2011. vol. 19, no. 5, pp. 698-706.

[9] SONI, V., SENKOV, O.N., GWALANI, B., MIRACLE, D.B. and BANERJEE, R. Microstructural design for improving ductility of an initially brittle refractory high entropy alloy. *Scientific Reports*. 2018. vol. 8, no. 1, p. 8816.

[10] SHEIKH, S., SHAFEIE, S., HU, Q., AHLSTRÖM, J., PERSSON, C., VESELÝ, J., ZÝKA, J., KLEMENT, U. and GUO, S. Alloy design for intrinsically ductile refractory high-entropy alloys. *Journal of Applied Physics*. 2016. vol. 120, no. 16, p. 164902.

[11] LI, X., TIAN, F., SCHÖNECKER, S., ZHAO, J. and VITOS, L. Ab initio-predicted micro-mechanical performance of refractory high-entropy alloys. *Sci. Rep*. 2015. vol. 5, p. 12334.

[12] LILENSTEN, L., COUZINIÉ, J.-P., BOURGON, J., PERRIÈRE, L., DIRRAS, G., PRIMA, F. and GUILLOT, I. Design and tensile properties of a bcc Ti-rich high-entropy alloy with transformation-induced plasticity. *Mater. Res. Lett*. 2017. vol. 5, pp. 110-116.

[13] YAO, J. Q., LIU, X., GAO, N., JIANG, Q.H., LI, N., ZHANG, W., FAN, Z.T. and LIU, G. Phase stability of a ductile single-phase BCC Hf0.5Nb0.5Ta0.5Ti1.5Zr refractory high-entropy alloy. *Intermetallics*. 2018. vol. 98, pp. 79-88.

[14] MORAVCIK, I. , GOUVEA, L., HORNIK, V., KOVACOVA, Z., KITZMANTEL, M., NEUBAUER, E.and DLOUHY, I. Synergic strengthening by oxide and coherent precipitate dispersions in high-entropy alloy prepared by powder metallurgy. *Scripta Materialia*. 2018. vol. 157, pp. 24-29.

[15] GOUVEA, L., MORAVCIK, I., CIZEK, J., KRAJNAKOVA, P., JAN, V. and DLOUHY, I. Characterization of powder metallurgy high-entropy alloys prepared by spark plasma sintering. *Materials Science Forum.* 2019. vol. 941, pp. 1053-1058.

[16] MORAVCIK, I., CIZEK, J., KOVACOVA, Z., NEJEZCHLEBOVA, J., KITZMANTEL, M., NEUBAUER, E., KUBENA, I., HORNIK, V. and DLOUHY, I. Mechanical and microstructural characterization of powder metallurgy CoCrNi medium entropy alloy. *Materials Science and Engineering: A*. 2017. vol. 701, pp. 370-380.

[17] MORAVCIK, I., GOUVEA, L., CUPERA, J. and DLOUHY, I. Preparation and properties of medium entropy CoCrNi/boride metal matrix composite. *Journal of Alloys and Compounds*. 2018. vol. 748, pp. pp. 979-988.